THE JOURNAL OF BIOLOGICAL CHEMISTRY VOL. 290, NO. 28, pp. 17566–17575, July 10, 2015
© 2015 by The American Society for Biochemistry and Molecular Biology, Inc. Published in the U.S.A.

Loss of α1,6-Fucosyltransferase Decreases Hippocampal Long Term Potentiation

*IMPLICATIONS FOR CORE FUCOSYLATION IN THE REGULATION OF AMPA RECEPTOR HETEROMERIZATION AND CELLULAR SIGNALING**

Received for publication, May 8, 2014, and in revised form, May 11, 2015 Published, JBC Papers in Press, May 15, 2015, DOI 10.1074/jbc.M114.579938

Wei Gu[‡], Tomohiko Fukuda[‡], Tomoya Isaji[‡], Qinglei Hang[‡], Ho-hsun Lee[‡], Seiichiro Sakai[§], Jyoji Morise[¶], Junya Mitoma[‖], Hideyoshi Higashi[‖], Naoyuki Taniguchi[**], Hiromu Yawo[§], Shogo Oka[¶], and Jianguo Gu[‡1]

*From the [‡]Division of Regulatory Glycobiology and the [‖]Division of Glyco-Signal Research, Tohoku Pharmaceutical University, Sendai, Miyagi, 981-8558, the [§]Graduate School of Life Sciences, Tohoku University, Sendai, Miyagi, 980-8577, the [¶]Department of Biological Chemistry, Human Health Sciences, Graduate School of Medicine, Kyoto University, Kyoto, 606-8507, and the **Disease Glycomics Team, RIKEN, Wako, Saitama 351-0198, Japan*

Background: High expression levels of core fucosylated *N*-glycans in brain tissues remain unexplained.
Results: Loss of core fucosylation enhanced AMPA receptor heteromerization and decreased long term potentiation.
Conclusion: Core fucosylation is required for hippocampal long term potentiation.
Significance: Core fucosylation may be very important for the neuronal synaptic plasticity that is required for learning and memory.

Core fucosylation is catalyzed by α1,6-fucosyltransferase (FUT8), which transfers a fucose residue to the innermost GlcNAc residue via α1,6-linkage on *N*-glycans in mammals. We previously reported that *Fut8*-knock-out (*Fut8*$^{-/-}$) mice showed a schizophrenia-like phenotype and a decrease in working memory. To understand the underlying molecular mechanism, we analyzed early form long term potentiation (E-LTP), which is closely related to learning and memory in the hippocampus. The scale of E-LTP induced by high frequency stimulation was significantly decreased in *Fut8*$^{-/-}$ mice. Tetraethylammonium-induced LTP showed no significant differences, suggesting that the decline in E-LTP was caused by postsynaptic events. Unexpectedly, the phosphorylation levels of calcium/calmodulin-dependent protein kinase II (CaMKII), an important mediator of learning and memory in postsynapses, were greatly increased in *Fut8*$^{-/-}$ mice. The expression levels of α-amino-3-hydroxy-5-methyl-4-isoxazolepropionate receptors (AMPARs) in the postsynaptic density were enhanced in *Fut8*$^{-/-}$ mice, although there were no significant differences in the total expression levels, implicating that AMPARs without core fucosylation might exist in an active state. The activation of AMPARs was further confirmed by Fura-2 calcium imaging using primary cultured neurons. Taken together, loss of core fucosylation on AMPARs enhanced their heteromerization, which increase sensitivity for postsynaptic depolarization and persistently activate *N*-methyl-D-aspartate receptors as well as Ca^{2+} influx and CaMKII and then impair LTP.

Schizophrenia is a common, chronic, and severe brain disorder that ranks as one of the leading causes of disability worldwide because it afflicts 2% of the world's population (1, 2). The disease is typically characterized by a loss of emotional expression and a lack of motivation. The etiology of schizophrenia is only partially understood, but multiepisode patients show significantly disturbed neuronal plasticity, suggesting that synaptic activity and connectivity are altered during the progression of the disease. Recently, cognitive impairments, such as deficits in learning and memory, have also been shown to be a fundamental feature of the disorder (3). Long term potentiation (LTP),[2] a well established model based on the neurophysiological study of learning and memory, has been found to be an important mechanism that underlies synaptic changes and plasticity in schizophrenia (4, 5). The induction of LTP begins with the activation of one kind of ionotropic glutamate receptor, α-amino-3-hydroxy-5-methyl-4-isoxazolepropionate receptors (AMPARs), which induce the opening of *N*-methyl-D-aspartate receptors (NMDARs), which are another kind of glutamate receptor, and leads to calcium entry that initiates a biochemical cascade through the activation of CaMKII, thereby increasing the number of AMPARs in the postsynaptic density (PSD) area. The end product of this biological reaction is the

* This work was supported in part by Grant-in-Aid for Scientific Research 21370059 (to J. G.) and Grants for Challenging Exploratory Research 23651196 (to J. G.) and 24590087 (to T. F.) from the Japan Society for the Promotion of Science. This work was also supported by Grant for Scientific Research on Innovative Areas 23110002 (to J. G.) and the Strategic Research Foundation Grant-aided Project for Private Universities from the Ministry of Education, Culture, Sports, Science, and Technology of Japan. The authors declare that they have no conflicts of interest with the contents of this article.

[1] To whom correspondence should be addressed: Division of Regulatory Glycobiology, Institute of Molecular Biomembrane and Glycobiology, Tohoku Pharmaceutical University, 4-4-1 Komatsushima, Aoba-ku, Sendai Miyagi, 981-8558, Japan. Tel.: 81-22-727-0216; Fax: 81-22-727-0078; E-mail: jgu@tohoku-pharm.ac.jp.

[2] The abbreviations used are: LTP, long term potentiation; E-LTP, early form LTP; AMPAR, α-amino-3-hydroxy-5-methyl-4-isoxazolepropionate receptor; CaMKII, calcium/calmodulin-dependent protein kinase II; GluA, a subunit of AMPARs; GluN, a subunit of NMDARs; HFS, high frequency stimulation; NMDAR, *N*-methyl-D-aspartate receptor; PSD, postsynaptic density; TARP, transmembrane AMPA receptor regulatory protein; TEA, tetraethylammonium.

long lasting potentiation of AMPAR-mediated excitatory postsynaptic current (6, 7).

Previous research has focused on identifying genes or protein expression-level changes in schizophrenia and ascertaining the functional effects of those alterations. Recently, the post-translational modification, *N*-glycosylation, has become a new target of investigation for schizophrenia (8). For example, abnormal *N*-glycans on AMPAR, NMDAR, and $GABA_A$ receptors were found in patients with schizophrenia (9–11).

The importance of fucosylation has been highlighted by the identification of the monogenetic inherited human disease, congenital disorder of glycosylation IIc (12). Due to defective Golgi GDP-fucose transporter activity, patients present with important clinical symptoms that include mental and growth retardation and severe immunodeficiency (13). Interestingly, the phenotypes of the transporter deletion mice (14) are similar to α1,6-fucosyltransferase knock-out (*Fut8*$^{-/-}$) mice (15), suggesting that core fucosylation is a key player among all fucosylations in mammals. Previously, we reported that the *Fut8*$^{-/-}$ mice exhibited multiple behavioral abnormalities, including decreased prepulse inhibition, increased locomotion, and impaired working memory with a schizophrenia-like phenotype (16). In fact, the unique structure of the core fucosylated *N*-glycans is highly expressed in brain tissues, and the expression patterns of *N*-glycans are altered during brain development (17).

To evaluate the effect of core fucosylation on LTP, we investigated synaptic strength and plasticity in the CA1 subregion of the hippocampus of *Fut8*$^{-/-}$ mice. We found that high frequency stimulation (HFS)-induced LTP was decreased in *Fut8*$^{-/-}$ mice. The molecular mechanism could have been caused by the aberrant heteromerization of AMPAR constitutively activating intracellular signaling, which may disturb LTP in *Fut8*$^{-/-}$ mice.

Experimental Procedures

Mice—The *Fut8*$^{-/-}$ mice were generated as described previously (16). All experiments were conducted with female and 3–5-week-old *Fut8*$^{-/-}$ and wild-type (*Fut8*$^{+/+}$) mice. The mice were housed in a temperature-controlled room with a 12-h dark/12-h light cycle and *ad libitum* feeding. This study was approved by the Institutional Animal Care and Use Committee of Tohoku Pharmaceutical University, Japan.

Antibodies and Reagents—Polyclonal antibodies against GluA1 and GluA2 (subunits of AMPAR) were obtained from Abcam; PSD95 was from Millipore; and GluA3, GluN2A, GluN2B (subunits of NMDAR), and CaMKII-α were from Cell Signaling. Rabbit monoclonal antibodies against GluN1, stargazin (TARP γ2), and synapsin-1 were from Cell Signaling. Monoclonal antibody against α-tubulin was from Sigma. Polyclonal antibodies against phosphorylated CaMKII at Thr-286, GluN2A at Tyr-1246, and GluN2B at Tyr-1472 all were obtained from Cell Signaling. Biotinylated *Aleuria aurantia* lectin was purchased from Seikagaku Corp. (Tokyo, Japan). *Pholiota squarrosa* lectin-Biotin conjugate agarose bead, which specifically recognizes core fucosylated *N*-glycans, was a generous gift from Dr. Kobayashi Yuka (J-Oil Mills, Inc., Tokyo, Japan). The magnetic protein A beads were from Invitrogen, and the avidin-biotin-agarose beads were from Millipore. Tetraethylammonium (TEA), kynurenic acid, and lidocaine all were obtained from Sigma. Glycine was purchased from Nacalai Tesque (Kyoto, Japan). L-Glutamic acid (glutamate), tetrodotoxin, 6-cyano-7-nitroquinoxaline-2,3-dione, and D-(−)-2-amino-5-phosphonopentanoic acid were purchased from Wako (Osaka, Japan).

Hippocampal Slice Preparation—Hippocampal slices (400 μm) were prepared from 3–5-week-old mice decapitated under isoflurance anesthesia. For the dissection, the cutting solution contained 229 mM mannitol, 3 mM KCl, 26 mM $NaHCO_3$, 1 mM H_3PO_4, 7 mM $MgCl_2$, and 11 mM glucose, pH 7.4, along with a mixed gas that was 95% O_2 and 5% CO_2, 1 mM kynurenic acid, and 200 μM lidocaine. For TEA-induced LTP recording, a surgical cut was additionally made between CA3 and CA1 to prevent epileptiform bursting. Slices were incubated at 34 °C for 1 h with artificial cerebrospinal fluid, which contained 125 mM NaCl, 2.5 mM KCl, 25 mM $NaHCO_3$, 1.25 mM NaH_2PO_4, 2 mM $CaCl_2$, 1 mM $MgCl_2$, 11 mM glucose, pH 7.4, with a mixed gas that was 95% O_2 and 5% CO_2. During the recording experiments, slices were superfused with an artificial cerebrospinal fluid flow (2 ml/min, 34 °C).

Extracellular Recordings and Induction of LTP—Field excitatory postsynaptic potentials were recorded in the stratum radiatum of the CA1 region using glass microelectrodes (tip diameters, 10 μm), which were filled with 1.78% Na_2SO_4 solution. A tungsten bipolar electrode was used to stimulate the Schaffer collateral axons and twin pulses at 200-μs duration and 50-ms intervals applied at a frequency of 0.033 Hz, with an intensity of less than 100 μA. The field excitatory postsynaptic potential was amplified and digitized using a conventional electrophysiological system (Axon Axopatch 200B plus Digidata1200B, Molecular Devices) and analyzed using Clampex version 10.2 software (Molecular Devices). A baseline recording was performed for at least 1 h. Then E-LTP was induced by applying a single 100-Hz train for 1 s at test strength. Voltage-dependent Ca^{2+} channel-dependent LTP was induced by applying 25 mM TEA for 10 min (18).

Ca^{2+} Imaging—Primary neural cells were cultured as described previously (19). After culturing for 14 days on glass-bottom dishes (Greiner Bio-one), the cultured media were replaced by a fresh medium containing 2 μM Ca^{2+} indicator Fura-2/AM (Dojindo, Japan) at 37 °C for 1 h to load and sensitize the probe by cleaving its AM group with cytosolic esterase. Fura-2-loaded cells were washed with a balanced salt solution, pH 7.4, consisting of 20 mM HEPES, 5.5 mM glucose, 130 mM NaCl, 5.4 mM KCl, 0.8 μM $MgSO_4$, and 1.8 μM $CaCl_2$. Indirect responses were blocked via the application of 1 μM tetrodotoxin in all procedures (20). Then cells were exposed to either 1 or 3 μM glutamate plus 10 μM glycine containing a balanced salt solution flow (1.75 ml/min, 34 °C) for 1 min, respectively, followed by a 3-min balanced salt solution flow wash. The AMPAR-mediated Ca^{2+} influx was blocked by an AMPA/kainate receptor antagonist, 6-cyano-7-nitroquinoxaline-2,3-dione or D-(−)-2-amino-5-phosphonopentanoic acid, a competitive NMDA receptor antagonist. The images were acquired at emission wavelengths between 490 and 520 nm while being excited sequentially at 340 (red) and 380 (green) nm (exposure time,

0.1–2 s). The ratio of F_{340}/F_{380}, indicating an influx efficiency of Ca^{2+}, was analyzed by using an image processor (Aqua Q, Hamamatsu, Japan) connected to a cooled CCD camera (Orca, Hamamatsu, Japan) (21).

Preparation of Hippocampus Extracts—Hippocampi were obtained from 3–5-week-old mice decapitated under isoflurance anesthesia. For Western blot, tissues were homogenized with modified radioimmune precipitation assay buffer consisting of 50 mM Tris-HCl, 1% Triton X-100, 0.2% sodium deoxycholate, 0.2% SDS, 1% protease inhibitor mixture (Nacalai Tesque), and 1% phosphatase inhibitor mixture (Nacalai Tesque). For immunoprecipitation, tissues were homogenized with 50 mM Tris-HCl plus 1% protease inhibitor mixture. Membrane fractions were sedimented by centrifugation (105,000 × *g*, 1 h, 4 °C) and dissolved in 1% Triton X-100, 50 mM Tris-HCl, 1 mM EDTA, and 1% protease inhibitor mixture for 45 min in a 37 °C water bath. After a subsequent removal of the insoluble materials by centrifugation, the supernatants were obtained for immunoprecipitation.

PSD Fractions—All biochemical experiments were carried out either on ice or at 4 °C (22). Dissected sections of mouse brains were homogenized with 10 volumes of buffer A (0.32 M sucrose, 10 mM Tris-HCl, 1 mM EDTA, and 1% protease inhibitor mixture) with 15 up and down strokes at 1,000 rpm. The homogenate was centrifuged at 1,000 × *g* for 10 min to remove the nuclear fraction and large debris. The supernatant (S1, postnuclear fraction) was centrifuged at 10,000 × *g* for 20 min to yield a crude synaptosome pellet (P2) and the supernatant (S2). The S2 was centrifuged at 105,000 × *g* for 60 min to yield a light membrane pellet (P3). The P2 fraction was lysed with hypo-osmotic (10% buffer A + 90% H_2O) buffer and centrifuged at 25,000 × *g* for 30 min to yield the synaptosomal membrane fraction (LP1). The LP1 fraction was then suspended in 0.5% Triton X-100 in buffer A for 15 min and centrifuged at 105,000 × *g* for 1 h to yield the PSD fraction. All pellet fractions were dissolved in 0.5% SDS. The protein concentration of each fraction was adjusted to 2 μg/μl using a Pierce BCA protein assay kit (Thermo).

Immunoblot Analysis and Immunoprecipitation—Cells cultured under different conditions were washed with PBS and lysed with lysis buffer that contained 1% Triton X-100, 10 mM Tris-HCl, 150 mM NaCl, and 1% protease inhibitor mixture. Cell lysates were separated in SDS-PAGE gels under reducing conditions and were then transferred to PVDF membranes. For Western blot, the membranes were blocked in 5% dried skimmed milk for 1 h at room temperature and probed with specific primary antibodies followed by incubation with appropriate secondary antibodies that had been conjugated with HRP. Finally, specific proteins were visualized using an ECL system (Amersham Biosciences). These membranes were stripped and reprobed with an antibody against the corresponding total proteins to confirm equal loading. For lectin blot, the membranes were blocked in 3% BSA and then detected with *A. aurantia* lectin. The immunoreactive bands were visualized using a Vectastain ABC kit (Vector Laboratories).

For the immunoprecipitation, all of the experiments were carried out on ice or at 4 °C; 2 μg of anti-GluA2 antibodies were attached to 5 μl of magnetic protein A beads in 100 μl of PBS plus 0.1% Triton X-100. Protein A beads were pelleted and incubated with the membrane lysates or cell lysates for 40 min with constant rotation. The beads were then washed three times with lysis buffer, and the immunoprecipitate was dissolved in 30 μl of SDS-PAGE sample solution.

Statistical Analysis—All of the electrophysiological data in this study are expressed as means ± S.E., and others are expressed as means ± S.D. Either a two-way analysis of variance or an unpaired Student's *t* test was used to analyze the statistical significance of these results.

Results

The Basal Synaptic Transmissions Were Increased, but HFS-induced LTP Was Decreased in Fut8$^{-/-}$ Mice—Previously, we reported that the *Fut8*$^{-/-}$ mice exhibited a schizophrenia-like phenotype (16). Synaptic activity and connectivity played important roles during the progression of the schizophrenia (3). Therefore, we analyzed basal synaptic neurotransmission. First, we recorded the field excitatory postsynaptic potential (*fEPSP*) in the hippocampus CA1 area (Fig. 1*A*) and found that the responses to stimuli were more sensitive in *Fut8*$^{-/-}$ mice than in *Fut8*$^{+/+}$ mice, which was confirmed by the input-output curve (Fig. 1*B*). However, the paired pulse ratio, which indicated presynaptic facilitation, showed no significant difference between *Fut8*$^{+/+}$ and *Fut8*$^{-/-}$ mice (Fig. 1*C*). On the other hand, based on our previous results from the Y-maze task, we knew that learning and memory could be impaired in *Fut8*$^{-/-}$ mice (16). We further examined the formation of E-LTP, which is generally used as a primary experimental model of memory formation in neuronal circuits. E-LTP was triggered by the application of HFS, and we found that the scale of E-LTP was significantly decreased in *Fut8*$^{-/-}$ mice, compared with *Fut8*$^{+/+}$ mice (Fig. 1*D*), but the TEA-induced (voltage-gated Ca^{2+} channel-dependent) LTP showed no significant difference (Fig. 1*E*), suggesting that the decline in the E-LTP in *Fut8*$^{-/-}$ mice was mainly caused by the events in postsynaptic neurons rather than in the presynaptic regions. Above all, *Fut8*$^{-/-}$ mice showed hyperactivity in basal synaptic transmissions and a decrease in E-LTP in postsynaptic neurons.

Persistent Activation of CaMKII and Increased AMPARs in the PSD Area of Fut8$^{-/-}$ Mice—To examine the events in the postsynaptic regions, we analyzed the activation levels of ionotropic glutamate receptors and CaMKII, which are mainly mediated in the induction and maintenance of E-LTP. We found that the CaMKII, a necessary component of the cellular machinery underlying learning and memory, was greatly activated in *Fut8*$^{-/-}$ mice (Fig. 2, *A* and *B*). Phosphorylation at Thr-286 of CaMKII plays essential roles in LTP, whereas LTP is attenuated in T286A (Thr-286 non-autophosphorylatable) mutant mice (23, 24). However, the expression of a constitutively active form of CaMKII into CA1 neurons enhances postsynaptic transmission and prevents further potentiation via synaptic stimulation (25, 26) because the CaMKII and LTP enhance synaptic transmission by the same mechanism (27). Thus, to be consistent with those observations, we thought that the persistent activation of CaMKII might lead to a decrease in E-LTP in *Fut8*$^{-/-}$ mice.

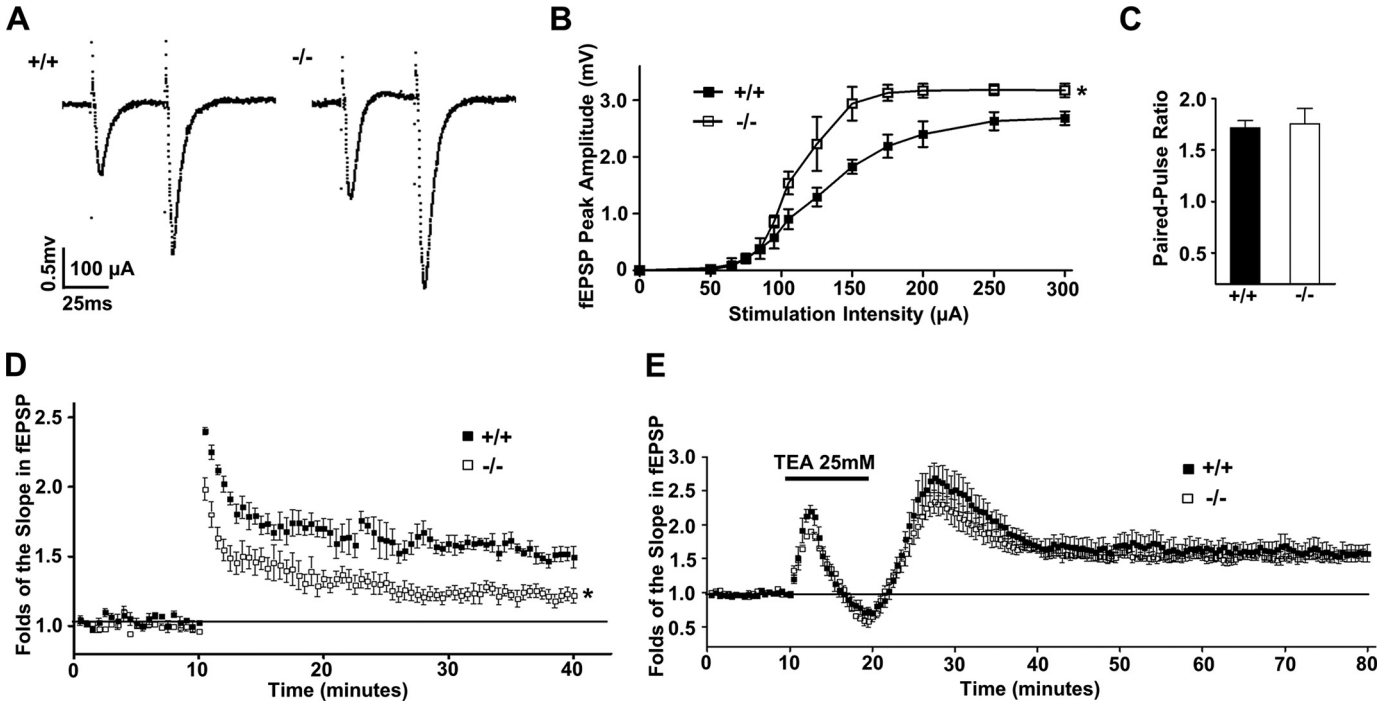

FIGURE 1. **The HFS-induced LTP was decreased in *Fut8*$^{-/-}$ mice, but L-Ca^{2+} channel-dependent LTP was not.** *A*, sample traces of field excitatory postsynaptic potential (*fEPSP*), induced by twin pulses at 200-μs duration and 50-ms intervals applied at a frequency of 0.033 Hz in 100 μA. *B*, ratio of stimulus intensity (input) to the amplitude of excitatory postsynaptic potential (output) (*Fut8*$^{+/+}$ ($N = 5, n = 12$) and *Fut8*$^{-/-}$ ($N = 6, n = 13$)). Data represent the mean $\pm$ S.E. *, $p < 0.05$, two-way analysis of variance. *C*, statistical comparisons of paired pulse ratio by unpaired Student's *t* test (mean $\pm$ S.D. (*error bars*)): 1.71 $\pm$ 0.07 ($N = 8, n = 20$) in *Fut8*$^{+/+}$ and 1.75 $\pm$ 0.15 ($N = 9, n = 22$) in *Fut8*$^{-/-}$. *D*, HFS was delivered after 10 min of baseline recording. HFS-induced LTP was recorded for another 30 min (*Fut8*$^{+/+}$ ($N = 6, n = 12$) and *Fut8*$^{-/-}$ ($N = 6, n = 12$)). Data represent the mean $\pm$ S.E. *, $p < 0.05$, two-way analysis of variance. *E*, 25 mM TEA was applied after baseline recording for 10 min. TEA-induced LTP was recorded for another 70 min. *Fut8*$^{+/+}$ ($N = 3, n = 7$) and *Fut8*$^{-/-}$ ($N = 3, n = 8$). Data represent the mean $\pm$ S.E. (*N*, number of mice; *n*, number of recordings).

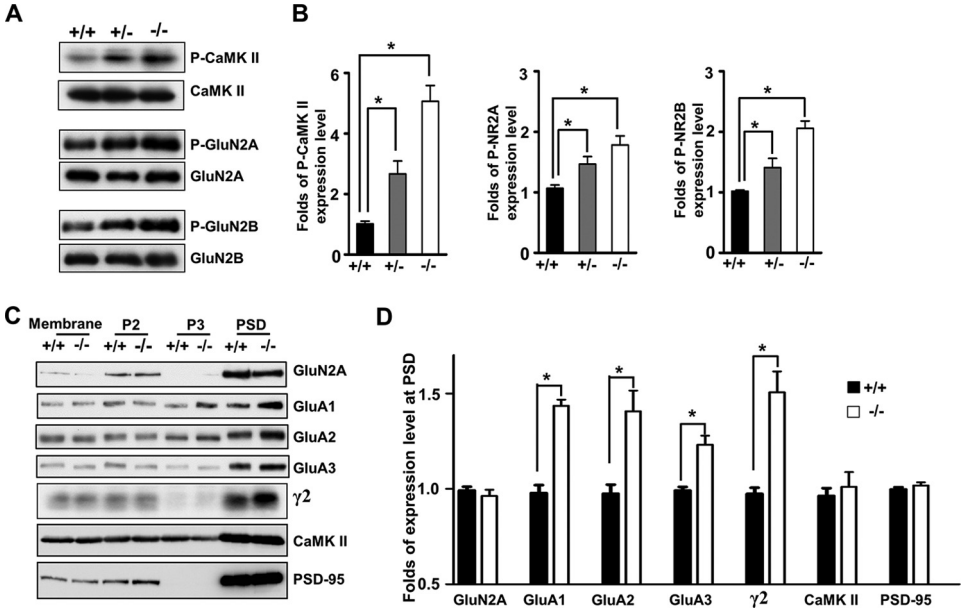

FIGURE 2. **Phosphorylated CaMKII levels were increased in *Fut8*$^{-/-}$ mice.** *A*, comparison of the phosphorylation of CaMKII, GluN2A, and GluN2B in the hippocampus of *Fut8*$^{+/+}$, *Fut8*$^{+/-}$, and *Fut8*$^{-/-}$ mice. *B*,, -fold P-CaMKII, P-GluN2A, and P-GluN2B expression levels are compared in *Fut8*$^{+/+}$ mice. The quantitative data were obtained from three independent experiments. Data represent the mean $\pm$ S.D. (*error bars*). *, $p < 0.05$, unpaired Student's *t* test. *C*, the PSD fraction was isolated by ultracentrifuge as described under "Experimental Procedures" and blotted with anti-GluN2A, anti-GluA1, anti-GluA2, anti-GluA3, anti-γ2, anti-CaMKII, and PSD-95. *P2*, crude synaptosome fraction; *P3*, light membrane fraction. *D*, -fold of expression levels of GluN2A, GluA1, GluA2, GluA3, γ2, CaMKII, and PSD-95 in PSD fraction of *Fut8*$^{-/-}$ mice, compared with those in *Fut8*$^{+/+}$ mice. The quantitative data were obtained from three independent experiments. Data represent the mean $\pm$ S.D. *, $p < 0.05$, unpaired Student's *t* test.

Ionotropic glutamate receptors, which can be subdivided into NMDAR, AMPAR, and kainate receptors, mediate most excitatory neuronal transmission (28). Among these receptors, NMDAR channels have several unique features, including a voltage-sensitive block by extracellular Mg^{2+} and a high permeability to Ca^{2+} (29). The Mg^{2+} block acts as a molecular

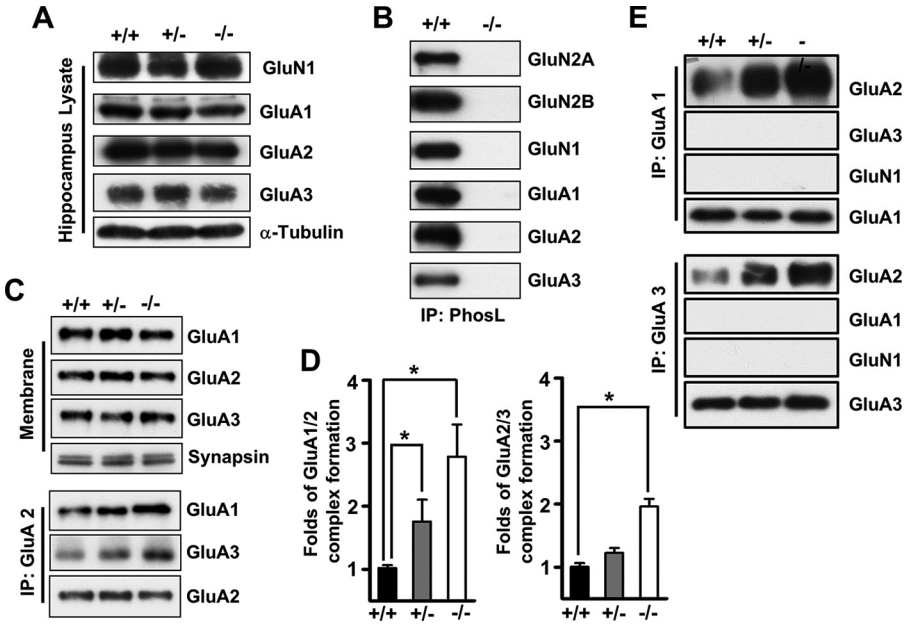

FIGURE 3. **Enhanced AMPAR heteromerization in *Fut8*$^{-/-}$ mice.** *A*, expression levels of GluN1 and GluAs between *Fut8*$^{+/+}$, *Fut8*$^{+/-}$, and *Fut8*$^{-/-}$ mice in hippocampus lysate. α-Tubulin was used as a loading control. *B*, comparison of core fucosylation levels on GluNs and GluAs between *Fut8*$^{+/+}$ and *Fut8*$^{-/-}$ mice. The same amounts of hippocampus lysates were immunoprecipitated (*IP*) with *P. squarrosa* lectin-agarose and blotted with anti-GluNs and anti-GluAs. *C*, membrane proteins were isolated as described under "Experimental Procedures." The same amounts of hippocampus membrane proteins were immunoprecipitated with anti-GluA2 and blotted with anti-GluA1, -GluA2, and -GluA3 (*bottom panels*). The total expression levels of GluA1, GluA2, and GluA3 and synapsin in hippocampus membranes were used as a loading control (*top panels*). *D*, -fold heteromerization levels of GluA1 and GluA2 (*right*) or GluA2 and GluA3 (*left*) were compared with those in *Fut8*$^{+/+}$ mice, which were set as 1. The quantitative data were obtained from three independent experiments. Data represent the mean ± S.D. (*error bars*); *, $p < 0.05$, unpaired Student's *t* test. *E*, the same amounts of hippocampus membrane proteins were immunoprecipitated with anti-GluA1 (*top panels*) or anti-GluA3 (*bottom panels*) antibodies and then blotted with anti-GluA2, anti-GluN1, and anti-GluA3 or anti-GluA1 antibodies, respectively.

switch, with the removal of Mg^{2+} from the pore of the channel when postsynaptic cells are depolarized. The relief of the block leads to the Ca^{2+} influx through the NMDAR channel that regulates synaptic strength through Ca^{2+}-activated signaling cascades. The phosphorylation of NMDAR is known to alter the channel properties (30). Consistent with the activated CaMKII in *Fut8*$^{-/-}$ mice, in the present study, the expression levels of phosphorylated GluN2A at Tyr-1246 and GluN2B at Tyr-1472 were also increased (Fig. 2, *A* and *B*). The rise of intracellular Ca^{2+} level causes reversible inactivation through the phosphorylation of receptors to prevent more synaptic stimulation (31). For example, phosphorylation of Tyr-1472, the major phosphorylation site by Fyn on GluN2B (32), disrupts its binding to an AP-2 adaptor, thereby resulting in the inhibition of GluN2B-mediated endocytosis.

When postsynaptic cells receive stimulation, the activated CaMKII phosphorylates TARPs binding to PSD95, thereby regulating AMPAR numbers in the PSD area (6, 33). However, with the decay of LTP, the AMPARs leave the PSD area and prepare for the next stimulation (7). The trafficking of AMPARs to regulate the number of receptors at the synapse plays a key role in various forms of synaptic plasticity. Interestingly, the expression levels of GluA1, GluA2, and GluA3, but not GluN2A and CaMKII, in the PSD area of brain tissues were increased in *Fut8*$^{-/-}$ mice (Fig. 2, *C* and *D*). Furthermore, Stargazin (γ2), the main member of the TARP family, accumulated in the PSD area and acted as auxiliary subunits of AMPARs (Fig. 2, *C* and *D*). The distribution of TARPs has been reported (33), γ2 is abundant throughout the brain, and γ8 is mainly expressed in the hippocampus. Unfortunately, we failed to detect subunits of γ8 using commercially available antibody.

The Enhanced Heteromerization of AMPARs in Fut8$^{-/-}$ *Mice*—To investigate the underlying mechanism of the persistent activation of CaMKII in *Fut8*$^{-/-}$ mice, we analyzed the heteromerization of AMPARs. Among the ionotropic glutamate receptors that mediate fast excitatory synaptic transmission, most of the biochemical cascades were initiated by the AMPAR-mediated depolarization of postsynaptic cells. Because AMPARs are the primary requirement in the expression of LTP, the modulation of AMPARs could affect synaptic transmission. In fact, several studies have reported that the biological functions of AMPARs are affected by post-translational modification (34). For example, human natural killer (HNK1) glycoepitope regulates the stability of GluA2 on the neuronal cell surface and dendritic spine maturation (22, 35). We found that there were no significant differences in either the total or the membrane expression levels of NMDARs and AMPARs in the hippocampi of the three genotypes of the mice (*Fut8*$^{+/+}$, *Fut8*$^{+/-}$, and *Fut8*$^{-/-}$) (Figs. 2*A*, 3*A*, and 3*C*), whereas the core fucosylation on these receptors was completely blocked in *Fut8*$^{-/-}$ mice (Fig. 3*B*). Then the heteromerization of AMPARs was analyzed by using a pull-down assay. The association levels of GluA1/2 and GluA2/3 were greatly increased in *Fut8*$^{-/-}$ mice compared with that in *Fut8*$^{+/+}$ mice (Fig. 3, *C–E*). Although it is well known that there are very few GluA1/3 complex formations in the hippocampus (36), the loss of core fucosylation could have altered the AMPAR complex formation. Thus, we checked the GluA1/3 complex formation as well as

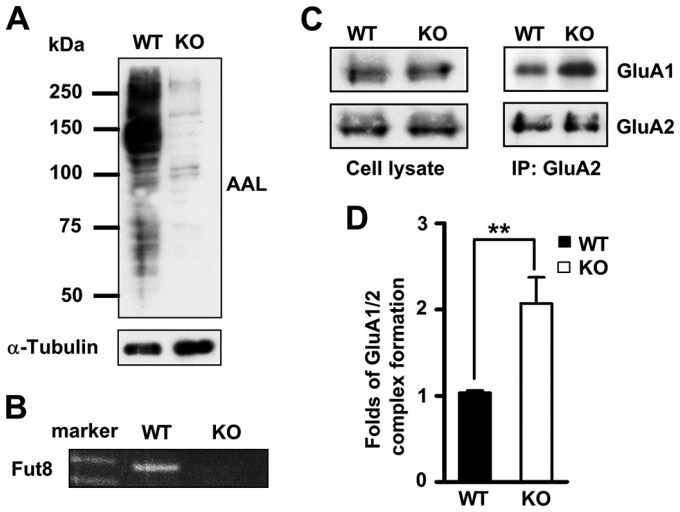

FIGURE 4. **Effect of core fucosylation on AMPAR heteromerization in 293T cells.** *A*, the *Fut8* gene was deleted by a KO technique using a CompoZr Knock-out Zinc Finger Nucleases (ZFN) kit (Sigma) in 293T cells according to the manufacturer's instructions. Equal amounts of 293T WT and *Fut8*-KO cell lysates were separated on 8% SDS-PAGE, and the membranes were probed with *A. aurantia* lectin, which specifically recognizes core fucose. α-Tubulin was used as a loading control. *B*, genomic DNA was extracted from 293T WT and *Fut8*-KO cells. The special primers were obtained from Sigma ZFN KIT and used to check for efficiency in the knock-out of *Fut8*. *C*, 293T WT and *Fut8*-KO cells were infected with GluA1 and GluA2 by Lipofectamine 2000 for 48 h. Total expression levels of GluA1 and GluA2 were imunoblotted with anti-GluA1 and anti-GluA2 antibodies (*left panels*). The same amounts of cell lysates were immunoprecipitated (*IP*) with anti-GluA2 (*right panels*) and blotted with anti-GluA1 and anti-GluA2 antibodies. *D*, -fold heteromerization levels of GluA1 and GluA2 in *Fut8*-KO cells compared with those in WT, which were set as 1. The quantitative data were obtained from three independent experiments. Data represent the mean ± S.D. (*error bars*); **, $p < 0.05$, Student's paired *t* test.

the interactions with GluA1. As shown in Fig. 3*E*, the levels of GluA1/3 complex formations could not be detected in the immunoprecipitates of either GluA1 (*top panels*) or GluA3 (*bottom panels*). Likewise, GluN1 expression was not detectable in either the GluA3 or GluA1 complexes. These data suggest that a loss of core fucosylation on AMPARs enhanced the heteromerization of their subunits, which might have subsequently depolarized the neuronal cell membrane to induce Ca^{2+} influx and CaMKII phosphorylation. Based on the observations in Fig. 3, *C* and *E*, we speculated that those heteromeric formations were mainly increased in the PSDs, as shown in Fig. 2*C*. Although the expression levels of homomeric receptors of membrane fractions in the KO mice were theoretically less than those in $Fut8^{+/+}$ or $Fut8^{+/-}$ mice, it is quite difficult to completely exclude the possibility that those homomeric receptors were also increased in $Fut8^{-/-}$ mice. In fact, it has been reported that homomeric GluA1 is first recruited into PSD following glutamate stimulation (37).

To further confirm the effects of core fucosylation on the complex formation for AMPARs, we expressed recombinant mouse GluA1 and GluA2 heteromeric combinations in wild-type and *Fut8*-knock-out (*Fut8*-KO) 293T cells, which were generated using the CompoZr Knock-out Zinc Finger Nucleases (ZFN) kit (Sigma), which was confirmed by an *A. aurantia* lectin blot (Fig. 4*A*) and RT-PCR (Fig. 4*B*). The coimmunoprecipitation experiments showed that the association levels of GluA1 and GluA2 were much higher in *Fut8*-KO cells compared with that in the wild-type 293T cells (Fig. 4, *C* and *D*). Taken together, these results strongly suggested that the loss of core fucosylation on AMPARs enhanced their subunit complex formation *in vitro*.

AMPAR-mediated Ca^{2+} Influx Was Enhanced in Primary Neurons Obtained from $Fut8^{-/-}$ Mice—Furthermore, to clarify the functions of the core fucosylation of AMPARs with respect to potentials, we examined the calcium influx in the 293T cells transfected with GluA1 alone compared with the cells co-transfected with GluA1 and GluA2. Unfortunately, when using the Fura-2 system, the induction of calcium influx upon glutamate stimulation was too small to measure in either the wild-type or the *Fut8*-KO 293T cells. Considering the possibility that an expression of NMDAR is required for the induction, we used primary cultured neurons as a model system to record the Ca^{2+} influx to examine the AMPAR and NMDAR potentials. Compared with primary neurons from $Fut8^{+/+}$ and $Fut8^{+/-}$ mice, the Ca^{2+} influxes were significantly increased in the neurons from $Fut8^{-/-}$ mice (Fig. 5, *A* and *B*). To check whether the increased Ca^{2+} influx in $Fut8^{-/-}$ was mediated by an AMPAR-NMDAR sequential response (38) (*i.e.* to determine whether AMPAR-induced postsynaptic depolarization can activate the NMDAR and then induce Ca^{2+} influx), both antagonists were added to the balanced salt solution bath flow. As shown in Fig. 5*C*, both 6-cyano-7-nitroquinoxaline-2,3-dione, an AMPAR blocker, and D-(−)-2-amino-5-phosphonopentanoic acid, a NMDAR inhibitor, could eliminate the difference in Ca^{2+} influx between $Fut8^{+/+}$ and $Fut8^{-/-}$ mice, further suggesting that the loss of core fucosylation enhances the heteromerization of AMPARs and their downstream signaling in primary cultured neurons.

Discussion

In the present study, we investigated the role of core fucosylation on E-LTP in the hippocampus and found that the HFS-induced LTP was dramatically decreased in $Fut8^{-/-}$ mice. A molecular mechanism could be postulated whereby the lack of core fucosylation in AMPARs results in aberrant heteromerization, which persistently activates cellular signaling, such as an increase in CaMKII phosphorylation levels at the basal level. Although the underlying molecular mechanism requires further study, it is reasonable to speculate that a persistent activation of CaMKII may interfere with some of the normal signal pathways (or feedback loops), which would decrease the response for LTP stimulation. In fact, the expression of a constitutively active form of CaMKII enhanced postsynaptic transmission and prevented further LTP (25). A similar phenomenon has also been observed in MAPK pathways. An activation of the MAPK/ERK cascade (short term) is commonly thought to be important for cell proliferation, but a persistently activated ERK (long term) reverses and down-regulates cell growth (39, 40).

Social dysfunction related to the loss of neocortical excitation/inhibition balance is an important symptom in schizophrenia (41). In the present study, we found an increase in synaptic transmission in the hippocampal CA1 area, which indicated that the balance of excitation/inhibition might be impaired in $Fut8^{-/-}$ mice. On the other hand, several studies

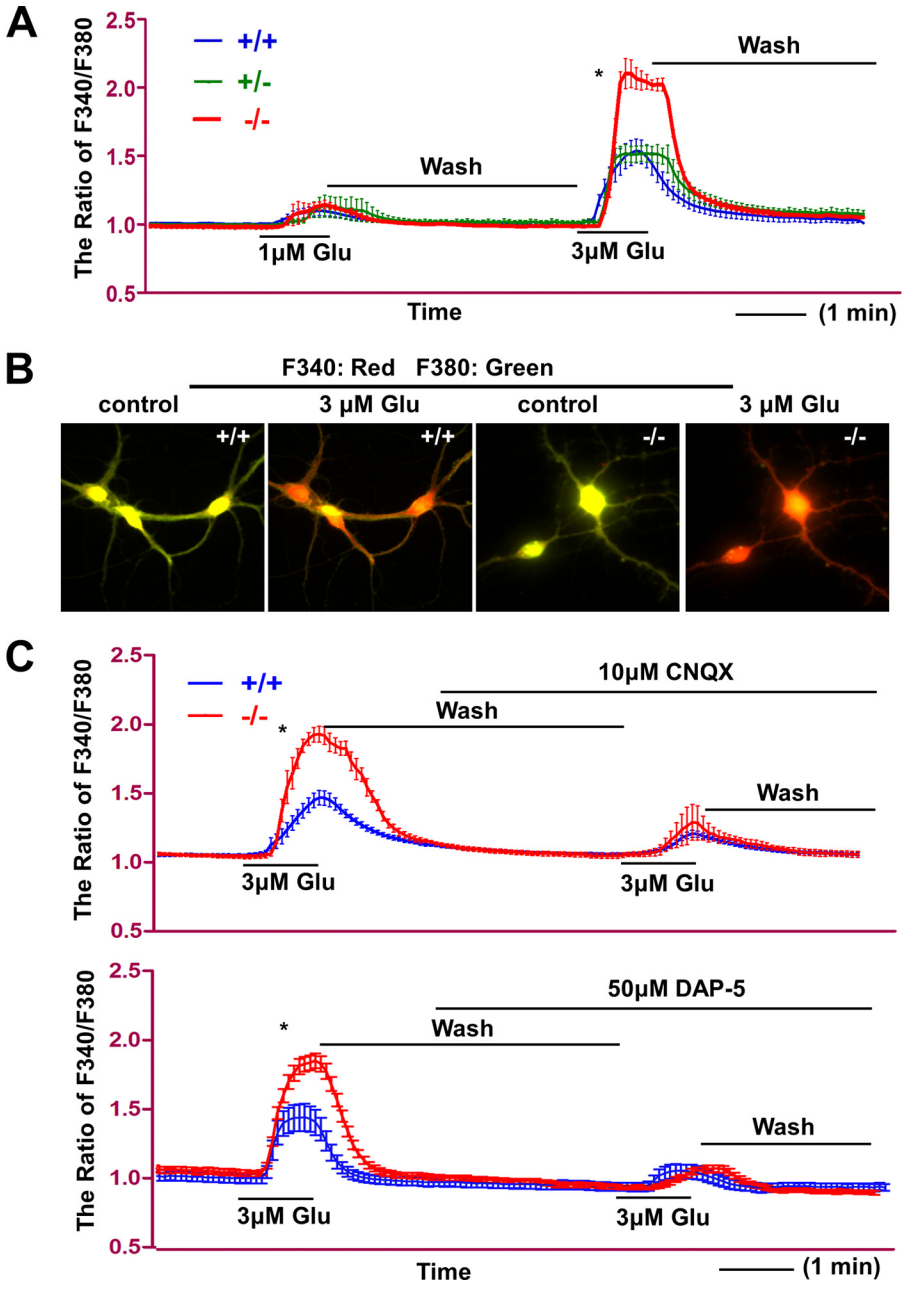

FIGURE 5. **AMPAR-mediated Ca^{2+} influx was enhanced in primary neurons from *Fut8*$^{-/-}$ mice.** *A*, primary neurons from *Fut8*$^{+/+}$, *Fut8*$^{+/-}$, and *Fut8*$^{-/-}$ mice cultured for 14 days *in vitro*. Cells were exposed to either 1 or 3 μM L-glutamic acid plus 10 μM glycine, respectively. The quantitative data were obtained from three independent experiments. One experiment comprised 40 cells in different fields of view. Data represent the mean ± S.E. An unpaired Student's *t* test was used for comparison of the peak reaction of independent groups; *, $p < 0.05$. *B*, a representative Ca^{2+} influx was visualized using an image processor connected to a cooled CCD camera. *control*, the image at baseline; *3 μM Glu*: the image of the peak during the stimulation of 3 μM L-glutamic acid plus 10 μM glycine. *C*, 6-cyano-7-nitroquinoxaline-2,3-dione (*CNQX*) or D-(−)-2-amino-5-phosphonopentanoic acid (*DAP-5*) was used to block the AMPAR-NMDAR-mediated Ca^{2+} influx. The quantitative data were obtained from three independent experiments. One experiment comprised 40 cells in different fields of view. Data represent the mean ± S.E. Student's unpaired *t* test was used for comparison of the peak reaction of independent groups; *, $p < 0.05$.

have provided direct neurophysiological evidence for disrupted LTP-like plasticity in schizophrenia (4, 5, 42). The evaluation of experimental LTP could be used to analyze the schizophrenia-like phenotype in *Fut8*$^{-/-}$ mice. It is well known that LTP is not a solitary phenomenon but contains various forms that can be categorized by the general mechanisms *in vivo*. For example, ionotropic glutamate receptors, metabotropic type glutamate receptors, and dopamine receptors (D1–D5) mediate LTP through different pathways (43). The LTP induced by HFS might be neither protein synthesis-dependent (D1–D5) nor metabotropic type glutamate receptor-dependent based on previous observations (43–45). Therefore, in the present study, we mainly focused on the molecules mediated in the ionotropic glutamate receptor-dependent pathway, including the NMDAR, AMPAR, and CaMKII in postsynaptic regions.

CaMKII activation plays essential roles in LTP because LTP induction that is produced by tetanus can be blocked by postsynaptic application of the peptide inhibitors of the kinase (46) or by a knock-in mutation that encodes T286A in CaMKII α (24). Based on these findings, we speculated that a decrease in

recorded LTP in *Fut8*$^{-/-}$ mice could be accompanied by a dysfunction in the activation of CaMKII. Unexpectedly, the phosphorylation levels of CaMKII in *Fut8*$^{-/-}$ mice were significantly higher than those in *Fut8*$^{+/+}$ mice (Fig. 2*A*). However, it is known that a constitutively active form of CaMKII is sufficient to augment synaptic strength and then prevents further tetanus-induced LTP (25). The hippocampal slices from *Fut8*$^{-/-}$ mice showed steeper input-output curves (Fig. 1*C*), which could strongly support potentiated synaptic transmission. Thus, we speculated that the absence of LTP in *Fut8*$^{-/-}$ mice could be due to a prior maximal activation rather than to a block of LTP. Altered hippocampal synaptic plasticity is likely to affect memory processing, and therefore any such pathology may contribute to the cognitive symptoms of schizophrenia. In a maternal immune activation animal model of schizophrenia, the enhanced persistence of dentate LTP has been associated with reduced behavioral flexibility, which may be related to the alteration of synaptic plasticity (3). In addition, Angelman disease, a form of intellectual disability, is associated with persistent activation of CaMKII, and a loss of LTP underlies this learning deficit in humans (47). These findings support our hypothesis that increased CaMKII activation in postsynaptic cells triggers LTP maximally and then prevents LTP induction, which may relate to the schizophrenia-like phenotype in *Fut8*$^{-/-}$ mice.

The AMPAR-mediated postsynaptic depolarization can activate the NMDAR, as well as Ca^{2+} influx and CaMKII. Curiously, the phosphorylated forms of NMDARs were greatly increased in *Fut8*$^{-/-}$ mice, compared with those in wild type mice (Fig. 2). This seems contradictory because the phosphorylated NMDARs suppress CaMKII activation (48). However, we speculated that a persistent CaMKII activation could promote the phosphorylation of NMDARs via a novel negative feedback mechanism to inhibit CaMKII activation. Therefore, the activation of AMPAR might determine the persistent activation of CaMKII in *Fut8*$^{-/-}$ mice. The ability of AMPARs to form a complex regulates their biological functions (49). Consistently, this heteromerization was greatly enhanced in the brain tissue of *Fut8*$^{-/-}$ mice, compared with that in *Fut8*$^{+/+}$ mice, which was further confirmed by the 293T overexpression system. Taken together, these studies strongly suggest that the enhanced AMPAR heteromerization may play a key role in augmenting the synaptic strength in *Fut8*$^{-/-}$ mice.

There are two major complex populations of AMPARs in adult hippocampal neurons: GluA1/2 and GluA2/3 (50). The GluA1/2 complex is recruited to dendritic spines in an activity-dependent manner, which is associated with CaMKII and requires an interaction with postsynaptic density proteins (35, 51). In contrast, GluA2/3 appears at the synapse, and its delivery is dependent on an interaction with cytoskeletal proteins, such as the *N*-ethylmaleimide-sensitive factor, and, therefore, GluA2/3 neurons are activated in a constitutively synaptic stimulation-independent manner (52). We focused on the function of the GluA1/2 complex in the present study because activity-dependent changes in the strength of excitatory synapses are the most important cellular mechanism for the plasticity of neuronal networks (53, 54). However, we did not exclude the possibility that the aberrant enhancement of the heteromerization of GluA2/3 might also contribute to a loss of LTP in *Fut8*$^{-/-}$ mice.

Furthermore, in CA1 pyramidal neurons, which serve as a model for understanding LTP, most receptors are known to exist as GluA1/2 heteromers with only a minor contribution from GluA2/3 complexes (36, 55). The enhancement of the heteromerization of GluA2 with GluA1 and GluA3 should generate calcium-impermeable low conductivity AMPARs and reduce both the general currents and the chances of postsynaptic depolarizations, resulting in a reduction in the LTP observed in *Fut8*$^{-/-}$ mice. It is clear that our observations in the present study could not be explained by the preceding notion. Based on the observation shown in Fig. 1, the basal transmission was increased in *Fut8*$^{-/-}$ mice, which suggests that the changes mainly occurred in the postsynaptic region. Furthermore, the phosphorylation levels of CaMKII were increased in *Fut8*$^{-/-}$ mice. Therefore, we speculated that an aberrant increase in GluA1/2 and GluA2/3 heteromeric formation induces a hypersensitive response for glutamate, which leads to the induction of postsynaptic depolarization, a persistent activation of NMDAR, and an increase in CaMKII phosphorylation levels, which might reverse and decrease the response for LTP stimulation in *Fut8*$^{-/-}$ mice, as discussed above.

The present study clearly demonstrated that a loss of core fucosylation could enhance the heteromerization of AMPARs and downstream signaling, but the molecular mechanism for the negative regulator of core fucosylation in the heteromerization remains unclear. Recently, two structural biology research groups analyzed the crystal structures of glycosylated FcγRIIIa and human core fucosylated or afucosylated Fc of IgG (56, 57). Interestingly, core fucose depletion can increase the incidence of the active conformation of the Tyr-296 of Fc, thereby accelerating the high affinity heteromerization with its receptor. Those studies clearly revealed why a lack of core fucosylation on IgG1 can dramatically enhance antibody-dependent cellular cytotoxicity activity (58, 59). In addition, some important amino acid residues in the N-terminal domains of AMPARs reportedly influence their biological functions by regulating the balance between the homo- and heteromeric associations (60). It should be noted here that the heteromeric formation of AMPAR is believed to take place in the endoplasmic reticulum (61), whereas core fucosylation occurs in the medial Golgi apparatus. The present finding that a loss of core fucosylation could enhance the heteromerization of AMPARs reflect the possibility that the regulation of AMPAR heteromerization could be in the Golgi network or at the cell surface as well as in the endoplasmic reticulum. We speculated that the presence of core fucose could have regulated the strength of the interaction in AMPAR complexes.

In fact, regulation of the AMPAR function is a complex process that involves many essential factors (53). For example, the TARP family members can associate with AMPARs and affect their expression levels in PSD, which would then regulate intracellular signaling for synaptic plasticity. Coincidentally, the higher expression levels of stargazin (TARP γ2) were increased in the PSD area in *Fut8*$^{-/-}$ mice (Fig. 2). The underlying molecular mechanism will require further study.

Recently, Tucholski *et al.* (9) reported that a high mannose type of *N*-glycans in AMPARs was significantly decreased in patients with schizophrenia, which, together with the results of the present study, further suggests that *N*-glycosylation can affect the functions of AMPARs. In conclusion, our study directly demonstrated the function of core fucosylation for learning and memory in hippocampal neurons, and the possible underlying mechanism for a schizophrenia-like phenotype was shown in *Fut8*$^{-/-}$ mice.

References

1. Freedman, R. (2003) Schizophrenia. *N. Engl. J. Med.* **349,** 1738–1749
2. Stanta, J. L., Saldova, R., Struwe, W. B., Byrne, J. C., Leweke, F. M., Rothermund, M., Rahmoune, H., Levin, Y., Guest, P. C., Bahn, S., and Rudd, P. M. (2010) Identification of *N*-glycosylation changes in the CSF and serum in patients with schizophrenia. *J. Proteome Res.* **9,** 4476–4489
3. Savanthrapadian, S., Wolff, A. R., Logan, B. J., Eckert, M. J., Bilkey, D. K., and Abraham, W. C. (2013) Enhanced hippocampal neuronal excitability and LTP persistence associated with reduced behavioral flexibility in the maternal immune activation model of schizophrenia. *Hippocampus* **23,** 1395–1409
4. Frantseva, M. V., Fitzgerald, P. B., Chen, R., Möller, B., Daigle, M., and Daskalakis, Z. J. (2008) Evidence for impaired long-term potentiation in schizophrenia and its relationship to motor skill learning. *Cereb. Cortex* **18,** 990–996
5. Sanderson, T. M., Cotel, M. C., O'Neill, M. J., Tricklebank, M. D., Collingridge, G. L., and Sher, E. (2012) Alterations in hippocampal excitability, synaptic transmission and synaptic plasticity in a neurodevelopmental model of schizophrenia. *Neuropharmacology* **62,** 1349–1358
6. Lisman, J., Yasuda, R., and Raghavachari, S. (2012) Mechanisms of CaMKII action in long-term potentiation. *Nat. Rev. Neurosci.* **13,** 169–182
7. Kullmann, D. M., and Lamsa, K. P. (2007) Long-term synaptic plasticity in hippocampal interneurons. *Nat. Rev. Neurosci.* **8,** 687–699
8. Khoury, G. A., Baliban, R. C., and Floudas, C. A. (2011) Proteome-wide post-translational modification statistics: frequency analysis and curation of the Swiss-Prot database. *Sci. Rep.* 10.1038/srep00090
9. Tucholski, J., Simmons, M. S., Pinner, A. L., Haroutunian, V., McCullumsmith, R. E., and Meador-Woodruff, J. H. (2013) Abnormal *N*-linked glycosylation of cortical AMPA receptor subunits in schizophrenia. *Schizophr. Res.* **146,** 177–183
10. Mueller, T. M., Haroutunian, V., and Meador-Woodruff, J. H. (2014) *N*-Glycosylation of GABAA receptor subunits is altered in schizophrenia. *Neuropsychopharmacology* **39,** 528–537
11. Tucholski, J., Simmons, M. S., Pinner, A. L., McMillan, L. D., Haroutunian, V., and Meador-Woodruff, J. H. (2013) *N*-Linked glycosylation of cortical *N*-methyl-D-aspartate and kainate receptor subunits in schizophrenia. *Neuroreport* **24,** 688–691
12. Etzioni, A., Frydman, M., Pollack, S., Avidor, I., Phillips, M. L., Paulson, J. C., and Gershoni-Baruch, R. (1992) Brief report: recurrent severe infections caused by a novel leukocyte adhesion deficiency. *N. Engl. J. Med.* **327,** 1789–1792
13. Sturla, L., Puglielli, L., Tonetti, M., Berninsone, P., Hirschberg, C. B., De Flora, A., and Etzioni, A. (2001) Impairment of the Golgi GDP-L-fucose transport and unresponsiveness to fucose replacement therapy in LAD II patients. *Pediatr. Res.* **49,** 537–542
14. Hellbusch, C. C., Sperandio, M., Frommhold, D., Yakubenia, S., Wild, M. K., Popovici, D., Vestweber, D., Gröne, H. J., von Figura, K., Lübke, T., and Körner, C. (2007) Golgi GDP-fucose transporter-deficient mice mimic congenital disorder of glycosylation IIc/leukocyte adhesion deficiency II. *J. Biol. Chem.* **282,** 10762–10772
15. Wang, X., Inoue, S., Gu, J., Miyoshi, E., Noda, K., Li, W., Mizuno-Horikawa, Y., Nakano, M., Asahi, M., Takahashi, M., Uozumi, N., Ihara, S., Lee, S. H., Ikeda, Y., Yamaguchi, Y., Aze, Y., Tomiyama, Y., Fujii, J., Suzuki, K., Kondo, A., Shapiro, S. D., Lopez-Otin, C., Kuwaki, T., Okabe, M., Honke, K., and Taniguchi, N. (2005) Dysregulation of TGF-β1 receptor activation leads to abnormal lung development and emphysema-like phenotype in core fucose-deficient mice. *Proc. Natl. Acad. Sci. U.S.A.* **102,** 15791–15796
16. Fukuda, T., Hashimoto, H., Okayasu, N., Kameyama, A., Onogi, H., Nakagawasai, O., Nakazawa, T., Kurosawa, T., Hao, Y., Isaji, T., Tadano, T., Narimatsu, H., Taniguchi, N., and Gu, J. (2011) α1,6-Fucosyltransferase-deficient mice exhibit multiple behavioral abnormalities associated with a schizophrenia-like phenotype: importance of the balance between the dopamine and serotonin systems. *J. Biol. Chem.* **286,** 18434–18443
17. Nakakita, S., Natsuka, S., Okamoto, J., Ikenaka, K., and Hase, S. (2005) Alteration of brain type *N*-glycans in neurological mutant mouse brain. *J. Biochem.* **138,** 277–283
18. Ohta, H., Sakai, S., Ito, S., Ishizuka, T., Fukazawa, Y., Kemuriyama, T., Tandai-Hiruma, M., Mushiake, H., Sato, Y., Yawo, H., and Nishida, Y. (2013) Paired stimulation between CA3 and CA1 alters excitability of CA3 in the rat hippocampus. *Neurosci. Lett.* **534,** 182–187
19. Gu, W., Fukuda, T., Isaji, T., Hashimoto, H., Wang, Y., and Gu, J. (2013) α1,6-Fucosylation regulates neurite formation via the activin/phospho-Smad2 pathway in PC12 cells: the implicated dual effects of Fut8 for TGF-β/activin-mediated signaling. *FASEB J.* **27,** 3947–3958
20. Padjen, A. L., and Smith, P. A. (1983) The role of the electrogenic sodium pump in the glutamate afterhyperpolarization of frog spinal cord. *J. Physiol.* **336,** 433–451
21. Kanatsu, Y., Chen, N. H., Mitoma, J., Nakagawa, T., Hirabayashi, Y., and Higashi, H. (2012) Gangliosides stimulate bradykinin B2 receptors to promote calmodulin kinase II-mediated neuronal differentiation. *J. Biochem.* **152,** 63–72
22. Morita, I., Kakuda, S., Takeuchi, Y., Itoh, S., Kawasaki, N., Kizuka, Y., Kawasaki, T., and Oka, S. (2009) HNK-1 glyco-epitope regulates the stability of the glutamate receptor subunit GluR2 on the neuronal cell surface. *J. Biol. Chem.* **284,** 30209–30217
23. Ohno, M., Frankland, P. W., and Silva, A. J. (2002) A pharmacogenetic inducible approach to the study of NMDA/αCaMKII signaling in synaptic plasticity. *Curr. Biol.* **12,** 654–656
24. Giese, K. P., Fedorov, N. B., Filipkowski, R. K., and Silva, A. J. (1998) Autophosphorylation at Thr286 of the α calcium-calmodulin kinase II in LTP and learning. *Science* **279,** 870–873
25. Pettit, D. L., Perlman, S., and Malinow, R. (1994) Potentiated transmission and prevention of further LTP by increased CaMKII activity in postsynaptic hippocampal slice neurons. *Science* **266,** 1881–1885
26. Pi, H. J., Otmakhov, N., Lemelin, D., De Koninck, P., and Lisman, J. (2010) Autonomous CaMKII can promote either long-term potentiation or long-term depression, depending on the state of T305/T306 phosphorylation. *J. Neurosci.* **30,** 8704–8709
27. Lledo, P. M., Hjelmstad, G. O., Mukherji, S., Soderling, T. R., Malenka, R. C., and Nicoll, R. A. (1995) Calcium/calmodulin-dependent kinase II and long-term potentiation enhance synaptic transmission by the same mechanism. *Proc. Natl. Acad. Sci. U.S.A.* **92,** 11175–11179
28. Dingledine, R., Borges, K., Bowie, D., and Traynelis, S. F. (1999) The glutamate receptor ion channels. *Pharmacol. Rev.* **51,** 7–61
29. Cull-Candy, S., Brickley, S., and Farrant, M. (2001) NMDA receptor subunits: diversity, development and disease. *Curr. Opin. Neurobiol.* **11,** 327–335
30. Wang, Y. T., Yu, X. M., and Salter, M. W. (1996) Ca^{2+}-independent reduction of *N*-methyl-D-aspartate channel activity by protein tyrosine phosphatase. *Proc. Natl. Acad. Sci. U.S.A.* **93,** 1721–1725
31. Medina, I., Filippova, N., Charton, G., Rougeole, S., Ben-Ari, Y., Khrestchatisky, M., and Bregestovski, P. (1995) Calcium-dependent inactivation of heteromeric NMDA receptor-channels expressed in human embryonic kidney cells. *J. Physiol.* **482**, 567–573
32. Takasu, M. A., Dalva, M. B., Zigmond, R. E., and Greenberg, M. E. (2002) Modulation of NMDA receptor-dependent calcium influx and gene expression through EphB receptors. *Science* **295,** 491–495
33. Payne, H. L. (2008) The role of transmembrane AMPA receptor regulatory proteins (TARPs) in neurotransmission and receptor trafficking (Review). *Mol. Membr. Biol.* **25,** 353–362
34. Jiang, J., Suppiramaniam, V., and Wooten, M. W. (2006) Posttranslational modifications and receptor-associated proteins in AMPA receptor trafficking and synaptic plasticity. *Neurosignals* **15,** 266–282

35. Kizuka, Y., and Oka, S. (2012) Regulated expression and neural functions of human natural killer-1 (HNK-1) carbohydrate. *Cell Mol. Life Sci.* **69,** 4135–4147
36. Wenthold, R. J., Petralia, R. S., Blahos, J., 2nd, and Niedzielski, A. S. (1996) Evidence for multiple AMPA receptor complexes in hippocampal CA1/CA2 neurons. *J. Neurosci.* **16,** 1982–1989
37. Tanaka, H., and Hirano, T. (2012) Visualization of subunit-specific delivery of glutamate receptors to postsynaptic membrane during hippocampal long-term potentiation. *Cell Rep.* **1,** 291–298
38. Guo, Z. Y., Li, C. Z., Li, X. J., Wang, Y. L., Mattson, M. P., and Lu, C. B. (2013) The developmental regulation of glutamate receptor-mediated calcium signaling in primary cultured rat hippocampal neurons. *Neuroreport* **24,** 492–497
39. Booth, A., Trudeau, T., Gomez, C., Lucia, M. S., and Gutierrez-Hartmann, A. (2014) Persistent ERK/MAPK activation promotes lactotrope differentiation and diminishes tumorigenic phenotype. *Mol. Endocrinol.* **28,** 1999–2011
40. Borrelli, E., Sawchenko, P. E., and Evans, R. M. (1992) Pituitary hyperplasia induced by ectopic expression of nerve growth factor. *Proc. Natl. Acad. Sci. U.S.A.* **89,** 2764–2768
41. Yizhar, O., Fenno, L. E., Prigge, M., Schneider, F., Davidson, T. J., O'Shea, D. J., Sohal, V. S., Goshen, I., Finkelstein, J., Paz, J. T., Stehfest, K., Fudim, R., Ramakrishnan, C., Huguenard, J. R., Hegemann, P., and Deisseroth, K. (2011) Neocortical excitation/inhibition balance in information processing and social dysfunction. *Nature* **477,** 171–178
42. Hasan, A., Nitsche, M. A., Rein, B., Schneider-Axmann, T., Guse, B., Gruber, O., Falkai, P., and Wobrock, T. (2011) Dysfunctional long-term potentiation-like plasticity in schizophrenia revealed by transcranial direct current stimulation. *Behav. Brain Res.* **224,** 15–22
43. Raymond, C. R. (2007) LTP forms 1, 2 and 3: different mechanisms for the "long" in long-term potentiation. *Trends Neurosci.* **30,** 167–175
44. Raymond, C. R., Thompson, V. L., Tate, W. P., and Abraham, W. C. (2000) Metabotropic glutamate receptors trigger homosynaptic protein synthesis to prolong long-term potentiation. *J. Neurosci.* **20,** 969–976
45. Bengtson, C. P., Freitag, H. E., Weislogel, J. M., and Bading, H. (2010) Nuclear calcium sensors reveal that repetition of trains of synaptic stimuli boosts nuclear calcium signaling in CA1 pyramidal neurons. *Biophys. J.* **99,** 4066–4077
46. Hvalby, O., Hemmings, H. C., Jr., Paulsen, O., Czernik, A. J., Nairn, A. C., Godfraind, J. M., Jensen, V., Raastad, M., Storm, J. F., and Andersen, P. (1994) Specificity of protein kinase inhibitor peptides and induction of long-term potentiation. *Proc. Natl. Acad. Sci. U.S.A.* **91,** 4761–4765
47. Weeber, E. J., Jiang, Y. H., Elgersma, Y., Varga, A. W., Carrasquillo, Y., Brown, S. E., Christian, J. M., Mirnikjoo, B., Silva, A., Beaudet, A. L., and Sweatt, J. D. (2003) Derangements of hippocampal calcium/calmodulin-dependent protein kinase II in a mouse model for Angelman mental retardation syndrome. *J. Neurosci.* **23,** 2634–2644
48. Chen, B. S., and Roche, K. W. (2007) Regulation of NMDA receptors by phosphorylation. *Neuropharmacology* **53,** 362–368
49. Sans, N., Vissel, B., Petralia, R. S., Wang, Y. X., Chang, K., Royle, G. A., Wang, C. Y., O'Gorman, S., Heinemann, S. F., and Wenthold, R. J. (2003) Aberrant formation of glutamate receptor complexes in hippocampal neurons of mice lacking the GluR2 AMPA receptor subunit. *J. Neurosci.* **23,** 9367–9373
50. Shi, S. H., Hayashi, Y., Petralia, R. S., Zaman, S. H., Wenthold, R. J., Svoboda, K., and Malinow, R. (1999) Rapid spine delivery and redistribution of AMPA receptors after synaptic NMDA receptor activation. *Science* **284,** 1811–1816
51. Sans, N., Racca, C., Petralia, R. S., Wang, Y. X., McCallum, J., and Wenthold, R. J. (2001) Synapse-associated protein 97 selectively associates with a subset of AMPA receptors early in their biosynthetic pathway. *J. Neurosci.* **21,** 7506–7516
52. Lynch, M. A. (2004) Long-term potentiation and memory. *Physiol. Rev.* **84,** 87–136
53. Derkach, V. A., Oh, M. C., Guire, E. S., and Soderling, T. R. (2007) Regulatory mechanisms of AMPA receptors in synaptic plasticity. *Nat. Rev. Neurosci.* **8,** 101–113
54. Malinow, R., and Malenka, R. C. (2002) AMPA receptor trafficking and synaptic plasticity. *Annu. Rev. Neurosci.* **25,** 103–126
55. Lu, W., Shi, Y., Jackson, A. C., Bjorgan, K., During, M. J., Sprengel, R., Seeburg, P. H., and Nicoll, R. A. (2009) Subunit composition of synaptic AMPA receptors revealed by a single-cell genetic approach. *Neuron* **62,** 254–268
56. Ferrara, C., Grau, S., Jäger, C., Sondermann, P., Brünker, P., Waldhauer, I., Hennig, M., Ruf, A., Rufer, A. C., Stihle, M., Umaña, P., and Benz, J. (2011) Unique carbohydrate-carbohydrate interactions are required for high affinity binding between FcγRIII and antibodies lacking core fucose. *Proc. Natl. Acad. Sci. U.S.A.* **108,** 12669–12674
57. Mizushima, T., Yagi, H., Takemoto, E., Shibata-Koyama, M., Isoda, Y., Iida, S., Masuda, K., Satoh, M., and Kato, K. (2011) Structural basis for improved efficacy of therapeutic antibodies on defucosylation of their Fc glycans. *Genes Cells* **16,** 1071–1080
58. Shields, R. L., Lai, J., Keck, R., O'Connell, L. Y., Hong, K., Meng, Y. G., Weikert, S. H., and Presta, L. G. (2002) Lack of fucose on human IgG1 *N*-linked oligosaccharide improves binding to human Fcγ RIII and antibody-dependent cellular toxicity. *J. Biol. Chem.* **277,** 26733–26740
59. Shinkawa, T., Nakamura, K., Yamane, N., Shoji-Hosaka, E., Kanda, Y., Sakurada, M., Uchida, K., Anazawa, H., Satoh, M., Yamasaki, M., Hanai, N., and Shitara, K. (2003) The absence of fucose but not the presence of galactose or bisecting *N*-acetylglucosamine of human IgG1 complex-type oligosaccharides shows the critical role of enhancing antibody-dependent cellular cytotoxicity. *J. Biol. Chem.* **278,** 3466–3473
60. Rossmann, M., Sukumaran, M., Penn, A. C., Veprintsev, D. B., Babu, M. M., and Greger, I. H. (2011) Subunit-selective *N*-terminal domain associations organize the formation of AMPA receptor heteromers. *EMBO J.* **30,** 959–971
61. Greger, I. H., Khatri, L., Kong, X., and Ziff, E. B. (2003) AMPA receptor tetramerization is mediated by Q/R editing. *Neuron* **40,** 763–774